Paper AAS 01-461

Automated Detection of Potentially Hazardous Near-Earth Encounters

Paul W. Chodas
Steven R. Chesley
Alan B. Chamberlin
Donald K. Yeomans

Jet Propulsion Laboratory
California Institute of Technology
Pasadena, California 91109

AAS/AIAA Astrodynamics Specialists Conference

Quebec City, Quebec, Canada July 30-August 2, 2001

AAS Publications Office, P.O. Box 28130, San Diego, CA 92198

AAS 01-461

AUTOMATED DETECTION OF POTENTIALLY HAZARDOUS NEAR-EARTH OBJECT ENCOUNTERS

Paul W. Chodas*
Steven R. Chesley*
Alan B. Chamberlin*
Donald K. Yeomans†

Over the last two decades, there has been an increasing public and scientific awareness of the impact hazard posed by Near-Earth Objects (NEOs). We have implemented an automatic process for updating orbital solutions for NEOs and detecting those objects that have an Earth collision probability greater than about 10^{-6}. Since some NEO orbits are very uncertain, nonlinearites can be large, and both Monte Carlo and multiple solutions methods are used for detecting possible Earth close encounters in these cases. Close approach data are collated and analyzed on the impact plane for each encounter. Automation using robust algorithms is essential because of the large number of objects and possible close approaches. This paper discusses the techniques and algorithms used, and presents a few examples of asteroids which for a time had significantly non-zero probabilities of colliding with the Earth. In most of these cases, subsequent observations led to more precise orbital solutions and eliminated the possibility of collision.

INTRODUCTION

Over the last two decades, there has been an increasing public and scientific awareness of the hazard posed by Near-Earth Objects (NEOs). Evidence has been gathered to support the claim that an extraterrestrial impact was responsible for large-scale extinctions at the boundary between the Cretaceous and Tertiary eras. More recently, evidence has been found to support the theory that the even larger mass extinction at the Permian-Triassic boundary resulted from an impact event. In response to increasing public and congressional interest, NASA has increased its funding of asteroid surveys, and adopted the goal of finding 90% of the kilometer-and-larger-sized asteroids by the year 2008. The latest population estimates for these objects indicate there are about a thousand of these objects; only 50 percent of them have been discovered to date. During the course of these surveys, many hundreds of smaller NEOs have been found, and hundreds of thousands remain to be found in the size range which would survive passage through the atmosphere, should any be on a collision course with Earth.

* Member of Technical Staff, Navigation and Mission Design Section, Jet Propulsion Laboratory, California Institute of Technology, Pasadena, California 91109. E-mail: paul.chodas@jpl.nasa.gov.
† Senior Research Scientist, Navigation and Mission Design Section, Jet Propulsion Laboratory, California Institute of Technology, Pasadena, California 91109.

Asteroids and comets are often categorized according to their orbital characteristics. To be called a Near-Earth Object an asteroid or comet must have a perihelion distance less than 1.3 AU (1 Astronomical Unit is equivalent to 149,597,871 km). The current number of known NEOs is about 1450, although most of these are relatively small. If we restrict the count to near-Earth asteroids larger than 1 km in size, the current number is about 500. Most of these objects cannot approach anywhere near the Earth except perhaps on million-year timescales. A more specialized category called the Potentially Hazardous Asteroids (PHAs) consists of those asteroids whose orbits approach within 0.05 AU (19.5 lunar distances) of the Earth's orbit, and whose size is at least 150 meters or so. The current number of known PHAs is about 310. Figure 1 shows the orbit of one of these, asteroid 1997 XF_{11}, which will make one of the closest predicted approaches to the Earth in 2028. The line of nodes shown in the diagram is the intersection of the orbit plane of the asteroid with the ecliptic plane. Close approaches are possible when an object crosses through its line of nodes near the Earth's orbit.

In order to evaluate the threat posed by known Near-Earth Objects, they must be tracked regularly, accurate orbits must be determined for each, and future close approaches must be predicted. At JPL, we have for decades computed the orbits for selected asteroids and comets, especially mission targets, and for several years, we have maintained an on-line database of NEO orbit solutions and close approach predictions. Recently, we have implemented an automated system for updating orbital solutions for NEOs and detecting those objects that have an Earth collision probability greater than about 10^{-6}. A similar system has been in operation at the University of Pisa for over a year [Ref: Chesley & Milani 2000DDA].

AUTOMATED ORBIT DETERMINATION FOR NEAR-EARTH OBJECTS

Orbits of asteroids and comets are determined primarily from ground-based astrometric observations, which consist of right ascension and declination coordinate pairs, together with the associated time tags and station coordinates. For newly discovered objects, only a handful of these observations may be available, while for well-observed objects, the data set may consist of hundreds or even thousands of observations. Modern optical astrometric observations have accuracies typically better than one arc-second, root-mean-square, with the dominant error source being the catalogued coordinates of the background reference stars used to compute the object coordinates. These observations are made by astronomers around the world, both professional and amateur, and are sent to the Minor Planet Center in Cambridge, Massachusetts, which serves as a clearinghouse for these data on behalf of the International Astronomical Union. Objects which are large enough and approach close enough to the Earth can also be observed using ground-based radar[1], which provides not only images of these objects, but also highly accurate measurements of echo delay and Doppler shift. The round-trip delay time can typically be measured to an accuracy corresponding to tens of meters in the range between the radar station and object.

In our automated process, new astrometric observations are automatically downloaded every day from the Minor Planet Center web site (http://cfa-www.harvard.edu/mpec/RecentMPECs.html). For newly discovered objects, a new observational data set is automatically created, and the preliminary orbit computed by the Minor Planet Center is also downloaded from the web site. For known objects, any new and/or corrected observations are automatically merged into the respective observational files. Sometimes, two known objects observed at widely different times are found to be one and the same, in which case the respective data sets are merged. New radar observations of NEOs obtained directly from observers are also merged into the observational data sets, and are archived on a JPL web site (http://ssd.jpl.nasa.gov/radar_data.html). In addition to these daily updates, the system automatically synchronizes with each monthly batch of Minor Planet Circular updates, which include new observations and new orbit updates for NEOs, as well as corrected observations.

The daily and monthly processing of NEO astrometric observations produces a list of objects for which updated orbits must be determined, and this too is performed automatically. The basic problem in orbit determination is to estimate an object's six orbital elements $\mathbf{x}$ at some epoch t_0, given a set of astrometric measurements $\mathbf{z}$ taken at times $t_1,\ldots, t_n$. The iterative process of differential corrections is used. At each step of the iteration, the problem is linearized about the current best estimate of the orbit, the equations of motion of the object are numerically integrated over the time span of the observations, and predicted observations are computed. An improvement to the orbit is then derived via the linear method of weighted least squares, which minimizes the weighted sum of squares of the observation residuals (the differences between the actual observations and predicted observations). The process is automatically iterated until convergence is detected. A sophisticated rejection algorithm is used for outlier observations, although manual overrides can be used to force the inclusion of selected observations. Upon completion, the orbit determination process produces an orbit estimate $\hat{\mathbf{x}}$ at an epoch within the time span of the observations, together with an associated covariance matrix $\mathbf{P}$, which describes the accuracy of the estimate. In solving the weighted least squares problem at the heart of this process, rather than using the standard normal-equation approach, we use a numerically more stable procedure called the square root information filter [Ref: Bierman]. This method produces an upper triangular square root information matrix $\mathbf{R}$, from which the covariance matrix is computed via the relation $\mathbf{P} = \mathbf{R}^{-1}\left(\mathbf{R}^{-1}\right)^T$.

The NEO orbital solutions generated by our automated system are tabulated daily on the JPL Near-Earth Object web site (http://neo.jpl.nasa.gov).

PREDICTION OF CLOSE APPROACHES AND LINEAR ANALYSIS OF CLOSE APPROACH UNCERTAINTIES

Once the object's orbit has been determined, its future Earth close approaches are predicted by numerically integrating the nominal orbit solution forward in time, monitoring the Earth-object distance, and detecting close approaches to within a threshold distance of 0.1 - 0.2 AU. In fact, close approaches to all perturbing bodies are detected, but only close approaches to the Earth are considered here. For objects with well-determined orbits, we propagate several centuries into the future, but for the majority of objects, we restrict the propagation to the next 50 to 100 years. The integrator used is a variable-order, variable-step Adams method, which adjusts the step size automatically so as to maintain a local velocity error of less than 10^{-13} AU per day. The Earth and Moon are considered as separate perturbers, rather than as a combined perturber located at the Earth-Moon barycenter. Perturbations by the three large asteroids Ceres, Pallas, and Vesta are included, and the general relativistic equations of motion are used. When the integrator senses a planetary close approach during a given step, it automatically interpolates within that step to find the precise close approach time, which is recorded along with the close approach distance.

In addition to predicting future close approaches of NEOs it is also important to compute the uncertainties in the close approach circumstances. An asteroid or comet's orbit cannot be known exactly, because the orbit calculation is based on imperfect measurements, and the uncertainty in the orbit estimate will produce uncertainties in the close approach predictions. A principal factor which determines the orbital accuracy of an asteroid or comet is the time span over which the object was observed, referred to as the *data arc*. A data arc of less than 10 days is very short, and will yield a fairly uncertain orbit; a data arc of a few months to a year would yield a moderately accurate orbit; and a data arc longer than the object's orbital period (typically a few years) should yield a fairly secure orbit. Secondary factors affecting the orbital accuracy include the number and precision of the observations, the object's proximity to the Earth when observed, and whether or not radar observations were used in the orbit solution.

The covariance matrix **P** is a measure of the uncertainty in an orbit solution, since it describes the multivariate Gaussian probability density function centered on the nominal solution in the space of initial orbital elements. The *confidence region* is the region about the nominal where orbital solutions are still reasonably consistent with the observations, as measured by a limiting number of standard deviations (sigmas). Under the assumption of linearity, this region is an ellipsoid (typically in 6-dimensional space), and we may speak, for example, of the 3-sigma confidence ellipsoid. If the confidence region is small enough (i.e. the orbit is reasonably well determined), then it is well approximated by the confidence ellipsoid.

The computation of the close approach circumstances is subject to an additional possible source of nonlinearity, namely the propagation from the epoch of the orbit solution (near the time of observation) to the epoch of the close approach. If the close approach is not too far in the future, and the object does not make intervening deep close

approaches to a perturbing body, then linearity can again be assumed. A linear covariance procedure can be used to map the orbit uncertainty at the time of the observations to position and velocity uncertainties at the predicted times of close approach. The mapping is accomplished by computing the state transition or mapping matrix $\mathbf{Y}(t) \equiv \partial \mathbf{r}(t)/\partial \mathbf{x}$ at the close approach time t_{CA}, where $\mathbf{r}$ is the heliocentric position vector. We compute this matrix via numerical integration of the so-called variational equations,

$$\ddot{\mathbf{Y}}(t) = \frac{\partial \ddot{\mathbf{r}}(t)}{\partial \mathbf{r}} \mathbf{Y}(t) + \frac{\partial \ddot{\mathbf{r}}(t)}{\partial \mathbf{v}} \dot{\mathbf{Y}}(t),$$

where the partials of $\ddot{\mathbf{r}}(t)$ are computed analytically. The variational equations are numerically integrated at the same time as the equations of motion.

At each close approach, the so-called *b*-plane, or *impact plane* is computed, this being the plane perpendicular to the incoming asymptote of the hyperbolic geocentric trajectory[Ref Kizner]. The main parameter of interest is the geocentric position $\mathbf{b}$ of the intercept of the incoming asymptote on the impact plane, which is called the *impact parameter*. The object will impact the Earth if the magnitude of $\mathbf{b}$ is less than the capture radius for the encounter, given by

$$r_c = r_p \sqrt{1 + \frac{2\mu}{r_p v_\infty^2}}$$

where r_p is the radius of the Earth, μ is the gravitational parameter of the Earth, and v_∞ is the hyperbolic excess velocity of the encounter. The two b-plane components of $\mathbf{b}$ are the first two of six b-plane elements $\mathbf{x}_b$. The square root covariance $\mathbf{S}_b$ of the b-plane elements may be computed by linearly mapping the orbital element square root covariance matrix $\mathbf{R}^{-1}$ via the state transition matrix and the Jacobian matrix for the transformation to b-plane elements:

$$\mathbf{S}_b = \left(\frac{\partial \mathbf{x}_b}{\partial \mathbf{r}} \mathbf{Y} + \frac{\partial \mathbf{x}_b}{\partial \mathbf{v}} \dot{\mathbf{Y}} \right) \mathbf{R}^{-1}.$$

The upper left 2×2 partition of $\mathbf{P}_b = \mathbf{S}_b \mathbf{S}_b^T$ describes the uncertainty in $\mathbf{b}$, a 2-dimensional marginal Gaussian probability density function displayed graphically as an uncertainty ellipse. Even if the nominal solution does not lead to an impact, an impact is possible if any part of the uncertainty ellipse intersects the Earth disk. The probability of impact is estimated by integrating this marginal probability density function over the Earth's disk via an efficient semi-analytic technique [Ref]. The third component of the b-plane elements is the linearized time of flight, and its uncertainty represents the uncertainty in the close approach time.

The resulting Earth close-approach data generated by the automated system are tabulated daily on the JPL Near-Earth Object web site (http://neo.jpl.nasa.gov), where they can be viewed in various sort orders: for example, by date, close-approach distance, or object name. The quantities tabulated include the close approach time and its

uncertainty, the nominal and minimum 3-sigma close approach distances, the number of sigmas by which the uncertainty ellipse must be scaled to yield a grazing impact, and the impact probability. The current closest predicted Earth approach is that of asteroid 1999 AN_{10} in the year 2027, with a miss distance of only 0.0026 AU.

MONTE CARLO ANALYSIS OF CLOSE APPROACHES

The linear analysis of close approach uncertainties described above may fail to adequately describe the true uncertainties if the initial orbit solution is moderately uncertain, or the predicted close approach is quite far in the future (i.e. the prediction period covers many orbits of the object), or if the object makes intervening close approaches to any perturbing body. The main problem is that the uncertainties grow too large over the prediction interval, and the assumption of linearity in computing $\mathbf{P}_b$ no longer applies. Under simple Keplerian motion, position uncertainty along the orbit grows linearly with time, while the uncertainty perpendicular to the orbit path remains fairly bounded, especially normal to the orbital plane. If the orbit solution is even moderately uncertain, then after several orbits of prediction, the confidence region may subtend a fair fraction of the orbital circumference, or even wrap around the entire orbit. This leads to numerous problems. Part of the uncertainty region may experience Earth close approaches which go undetected because the nominal trajectory never approaches within the threshold distance of the Earth. In addition, even if the occurrence of a close approach is properly detected, the part of the uncertainty region nearest the Earth may be so far from the nominal that linearity within the b-plane does not apply. Finally, some portions of the uncertainty region may experience localized close approaches, producing significant nonlinearities in the uncertainty region.

Monte Carlo techniques offer a robust approach for exploring the diverse set of possible trajectories which evolve from a domain of orbit solutions at an initial epoch. We have implemented two variations of the Monte Carlo technique for detecting possible close encounters with the Earth. In the first approach, the six-dimensional ellipsoid representing the uncertainty of the orbital elements at epoch is randomly sampled with thousands of test points to create a set of initial conditions which are all then numerically integrated forward in time and the close approaches recorded [Ref M&B, C&Y-SL9]. [The sample points are sometimes referred to as *virtual asteroids* (VAs), since they follow the same equations of motion as the real object.] The samples are easily generated by applying a standard Gaussian random number generator to the square root covariance matrix, and adding to the nominal solution [Ref:Girdwood]. Since they are all equally likely, the samples are denser near the nominal solution, where the probability density reaches a maximum, and become progressively sparse away from the nominal.

A second variation of the Monte Carlo technique must be used if the confidence region in orbital element space is not well represented by the linear confidence ellipsoid, as in the case of objects with very uncertain orbits. With this approach, sample points are created by going back to the observations themselves and adding random noise vectors

according to the assumed observation error model. The orbit determination process is then applied to each sample set of modified observations, and the resulting orbit solutions become the sample points. Under this approach, the ensemble of samples will populate the actual confidence region, whatever its shape. Although this method is more computationally expensive than the first, it is generally needed only when the observational data arc is short (typically less than 30 days), and in these cases, the numerical integration required by the orbit determination process is relatively quick.

Regardless of which Monte Carlo variation is used, the numerical integration of the sample points can yield hundreds or thousands of close approach detections to within a threshold distance of 0.1 - 0.2 AU. The times of these close approaches are recorded, along with the geocentric position and velocity vectors. When the close approaches of the samples are collated by time, they cluster around separate encounter times, for example when the Earth passes close to the asteroid's nodal crossing point with the asteroid nearby. We refer to the set of points which experience a close approach around a given encounter time as a *shower*, since the concept is reminiscent of a meteor shower. Sometimes the entire set of samples form a shower, but more typically the confidence region is so spread out along the orbit that only a small subset of samples passes within the threshold distance.

In order to perform a two-dimensional analysis of each encounter, the close approaches are then projected into a common b-plane for that encounter. To ensure accuracy for cases approaching closest to the Earth, the b-plane is computed from the trajectory of the case which makes the closest approach of the encounter. The figure of the Earth in this plane will be a disk centered at the origin, with radius equal to the encounter capture radius r_c. (However, in some cases, we scale the b-plane diagrams by r_p / r_c so that the Earth disk has radius r_p.) A straightforward estimate of the impact probability for the encounter is simply the ratio of the number of samples which lie within the Earth disk to the total number of samples. Of course, this method will not yield a satisfactory result if the number of points on the Earth disk is small. In this case, the more sophisticated method described below must be used.

As an illustrative example of the Monte Carlo technique, we consider the case of asteroid 1997 XF_{11}, which made the news in March 1998 because of a prediction that it would make an extremely close approach to Earth in the year 2028, and a widely misunderstood statement that a collision was "not entirely out of the question" [Ref Marsden]. Even before pre-discovery observations from 1990 were found, a linear analysis of the impact probability showed that the chance of collision in 2028 was essentially zero, and the inclusion of the 1990 observations only served to confirm this fact [Chodas&Yeomans G&C]. It was later suggested, however, that *prior to the inclusion of the 1990 observations in the data set* (a somewhat hypothetical case), there was in fact a small possibility that 1997 XF_{11} could collide with the Earth in the decade or so after 2028 because the deep close approach in 2028 could alter the asteroid's orbital period in such a way as to bring it back even closer to Earth several orbits later [Marsden]. Linear methods were completely inadequate to analyze these later collision

possibilities because of the strong nonlinearity in the motion introduced by the 2028 close approach. The Monte Carlo technique, on the other hand, could handle the analysis, and was used to confirm that an impact in 2040 was indeed possible, with a probability on the order of 10^{-5} [Ref: Girdwood].

Figures 2 through 6 show the evolution of the confidence region for this hypothetical 1997 XF_{11} case through the 2040 encounter. Figure 2 shows 500 sample points populating the confidence ellipsoid at the epoch of the observations in 1998. The region is about 54,000 km in length and oriented towards the Earth. Figure 3 shows the confidence region thirty years later in 2028, when the nominal solution makes a close approach about 90,000 km north of the Earth center. The region has grown to a length of almost 3 million kilometers, but no part of the region passes closer than about 28,000 km to the Earth. The deep close approach heavily perturbs the linear confidence region into a loop, depicted in Figure 4, which shows the sample points 3 days after closest approach. The small kink in the right part of the confidence region is actually a loop caused by a close approach to the Moon. Figure 5 shows the situation two months later, when the confidence region loop has grown to a diameter of about 9 million kilometers (for scale, note the size of the Moon's orbit). A year after the 2028 close approach, the loop has stretched to a size of about 1 AU, as shown in Figure 6. Finally, in 2040, after 12 years, the confidence region extends almost completely around the orbit, as shown in Figure 7, and has broken further due to intervening close approaches to the Earth.

Although it cannot be seen in Figure 7, part of the confidence region for this hypothetical 1997 XF_{11} case cuts right across the Earth's disk. Figure 8 shows the result when a much larger set of Monte Carlo samples for this case are similarly propagated to 2040 and projected into the b-plane for that encounter. Points lying within the central circle represent Earth impacts: 12 cases impacted out of 600,000. The two points below the main group of points in Figure 8 took a different dynamical path to the 2040 encounter, passing the Earth in 2028 much closer than the points in the main group. These originated from a different part of the confidence region, and are more highly stretched by the 2028 encounter. We use the term *stream* to refer to the different subsets of samples which have followed qualitatively different dynamical paths to the encounter. The impact plane for the 2041 encounter is shown in Figure 9. In this case, four streams are evident as offset tracks of points, two main streams and two highly stretched secondary streams. One main stream and one secondary clearly cross the Earth, while the other main stream just grazes it.

The streams for an encounter must be analyzed separately, since each has a separate impact probability. One heuristic method of separating Monte Carlo sample points into separate streams is to sort and index them according to their initial semimajor axis, as each stream typically has a characteristic value. A more robust method will be discussed in the next section.

Once the samples have been separated into streams, we need to find the minimum possible close approach of the stream to the Earth. Starting from two points on either

side of the Earth disk, we compute the closest point along the line between them. We then obtain a new sample by linearly interpolating to the corresponding point along the line in orbital element space between the initial elements for the original two points. This procedure can then be iterated to convergence. If the resulting minimum possible close approach distance of a stream is less than one Earth radius, then we know that an impact is possible for this stream.

The secondary stream in Figure 8 passes no closer than 14,000 km from the Earth's center, and we might therefore conclude that this stream cannot impact. But in fact, it is necessary to compute the width of the confidence region at the minimum close approach point. This can be accomplished by performing a linear analysis about this point and computing the width of the target plane confidence ellipse. If the confidence region is much narrower than the diameter of the Earth disk, as is the case for highly stretched streams, a simple one-dimensional method can be used. For example, the impact probability can be estimated by computing the linear density of points over a domain centered on the origin, and multiplying by the chord length of the stream's Earth crossing. If the width of the target plane confidence region is not negligible with respect to the diameter of the Earth disk, two-dimensional methods must be used to compute the impact probability [Ref: Girdwood].

Finally, we reiterate that the above analysis was based on a *reduced* observation data set for 1997 XF_{11} because that was such an interesting case. We have performed a similar non-linear Monte Carlo analysis using the full set of observations for this asteroid, and conclude that 1997 XF_{11} has no significant chance of colliding with Earth for at least a century.

LINE OF VARIATION ANALYSIS OF CLOSE APPROACHES

While the Monte Carlo method samples the confidence region in a random way, another technique called the Method of Multiple Solutions [Ref] samples the region in a systematic order, which simplifies many of the algorithms for analyzing the close approaches. Furthermore, like our second variation of the Monte Carlo technique, this method can be used even if the confidence region in orbital element space is large and not adequately represented by the linear confidence ellipsoid. Typically the region has one long dimension in 6-dimensional space and is slightly curved. The important characteristic of this new method is that it samples only the main axis of the confidence region, which is called the Line of Variations. Starting at the nominal solution, this method consists of taking small steps of constant sigma value along the eigendirection associated with the largest eigenvalue of the covariance matrix. At each step point, the orbit and covariance matrix are re-determined, but the solution is constrained to lie in the plane perpendicular to the eigendirection. In this way, a series of solutions are obtained which essentially follow the main axis of the confidence region away from the nominal case. Stepping continues in both directions away from the nominal until the rms of the residuals reaches a 4-sigma value. For example, with a sampling step size of

0.001 standard deviations, this method yields a set of 8000 samples along the line of variations.

Once the sample points have been generated, they are numerically integrated forward in time, as before, and all the close approaches within the threshold distance are recorded. The close approach data are then sorted by time and separated into showers, as with the Monte Carlo techniques. In splitting the shower into separate streams, the algorithm can exploit the fact that the samples are ordered: streams are easily detected as sequences of consecutive samples within the same shower. The analysis performed on each stream to find the minimum possible close approach point, the width of the confidence region, and finally the impact probability is much the same as described above.

Figure 10 shows an example of the use of line of variations sampling. In this case we consider the encounter of lost asteroid 1998 OX_4, which was observed for only 9 days in 1998 and therefore has a very uncertain orbit. By the year 2046, this asteroid's confidence region has wrapped almost three times around the orbit. After the line of variations was populated with samples at a step size of 0.001 sigmas, the points were propagated to 2046, and projected into the b-plane. Four streams with multiple points were detected, but only one highly stretched stream with a total of eight points cuts across the Earth's disk. The impact probability for this stream is on the order of 10^{-6}. The lowest of the four streams is unlike the other three in that its sequence of points folds back upon itself. Special methods are required to analyze the impact probability of such *interrupted streams*, especially those which have folding points near the Earth.

ACKNOWLEDGEMENT

The research described in this paper was carried out by the Jet Propulsion Laboratory, California Institute of Technology, under contract with the National Aeronautics and Space Administration.

REFERENCES

1. Yeomans, D.K., P.W. Chodas, M.S. Keesey, and S.J. Ostro, "Asteroid and Comet Orbits Using Radar Data," *Astron. J.* **103**, 1992, pp. 303-317.

2. Chodas, P.W., and D.K. Yeomans, "Orbit Determination and Estimation of Impact Probability for Near-Earth Objects", Paper AAS 99-002, AAS Guidance and Control Conference, Breckenridge, Colorado, February 3-7, 1999.

3. Chodas, P.W., and D.K. Yeomans, "Predicting Close Approaches and Estimating Impact Probabilities for Near-Earth Objects", Paper AAS 99-462, AAS/AIAA Astrodynamics Specialist Conference, Girdwood, Alaska, August 16-19, 1999.

4. Bierman, G.J., *Factorization Methods for Discrete Sequential Estimation*, Academic Press, New York, 1997.

5. Near Earth Object Program web site, `http://neo.jpl.nasa.gov/`, Jet Propulsion Laboratory, Pasadena, California.

6. Yeomans, D.K., and P.W. Chodas, "Predicting Close Approaches of Asteroids and Comets to Earth," in *Hazards due to Comets and Asteroids*, T. Gehrels, ed., U. of Arizona Press, 1994, 241-258.

7. Muinonen, K., "Asteroid and Comet Encounters with the Earth," in *Proceedings of The Dynamics of Small Bodies in the Solar System: A Major Key to Solar System Studies*, A.E. Roy and B. Steves, eds., Kluwer, 1999.

9. Muinonen, K., and E. Bowell, "Asteroid Orbit Determination using Bayesian Probabilities," *Icarus* **104**, 1993, pp. 255-279.

10. Chodas, P.W., and D.K. Yeomans, "The Orbital Motion and Impact Circumstances of Comet Shoemaker-Levy 9," in *The Collision of Comet Shoemaker-Levy 9 and Jupiter*, K.S. Noll, H.A. Weaver, and P.D. Feldman, eds., Cambridge University Press, 1996.

11. Marsden, B.G., "A Discourse on 1997 XF11," *J. Brit. Interpl. Soc.* **52**, 1999, 195-202.

12. Milani, A., S.R. Chesley, and G.B. Valsecchi, "Close Approaches of Asteroid 1999 AN_{10}: Resonant and Non-resonant Returns," *Astron. Astrophys.* **346**, 1999, L65-L68.

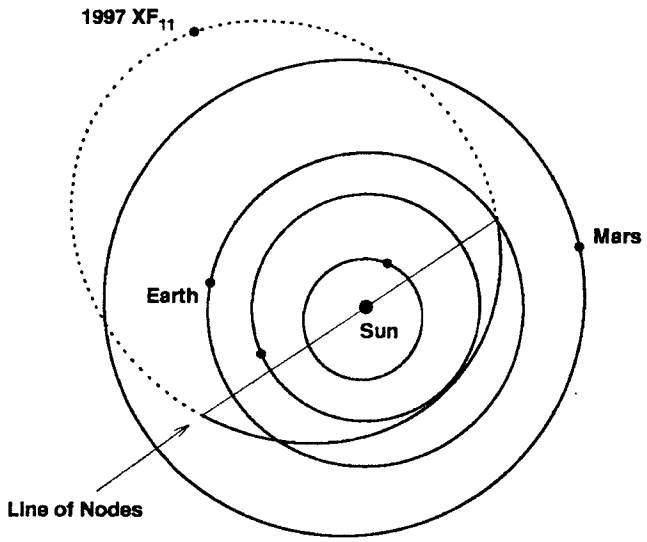

Figure 1 Orbit of Asteroid 1997 XF_{11}
(Orbit inclined 4.1° to ecliptic plane; dotted portion below ecliptic)

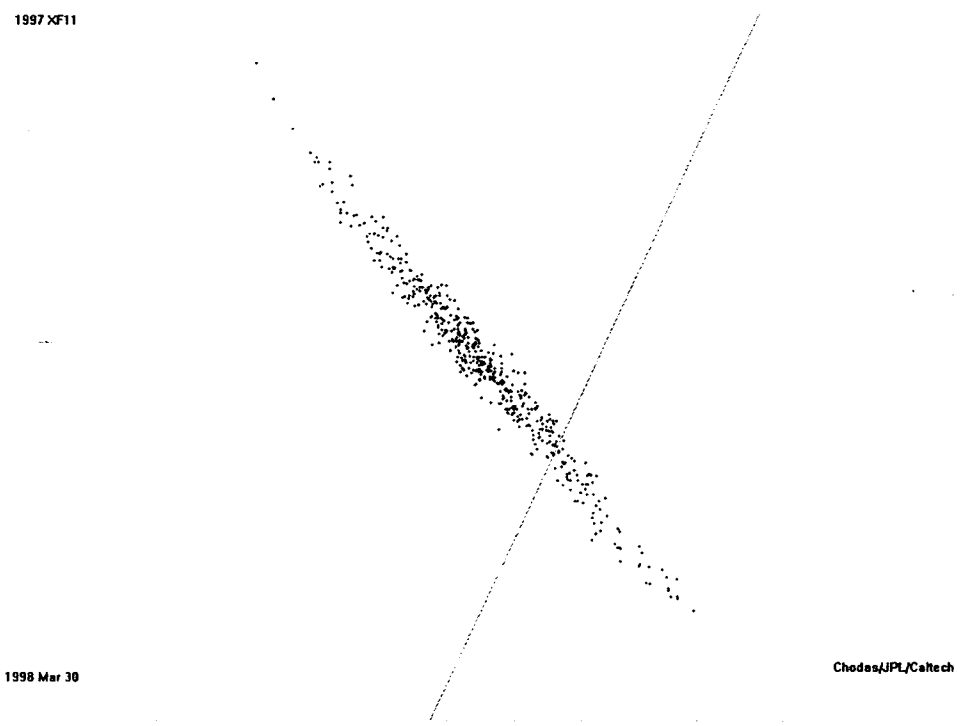

Figure 2 Positions of Monte Carlo points for 1997 XF_{11}
at epoch of last observation in 1998

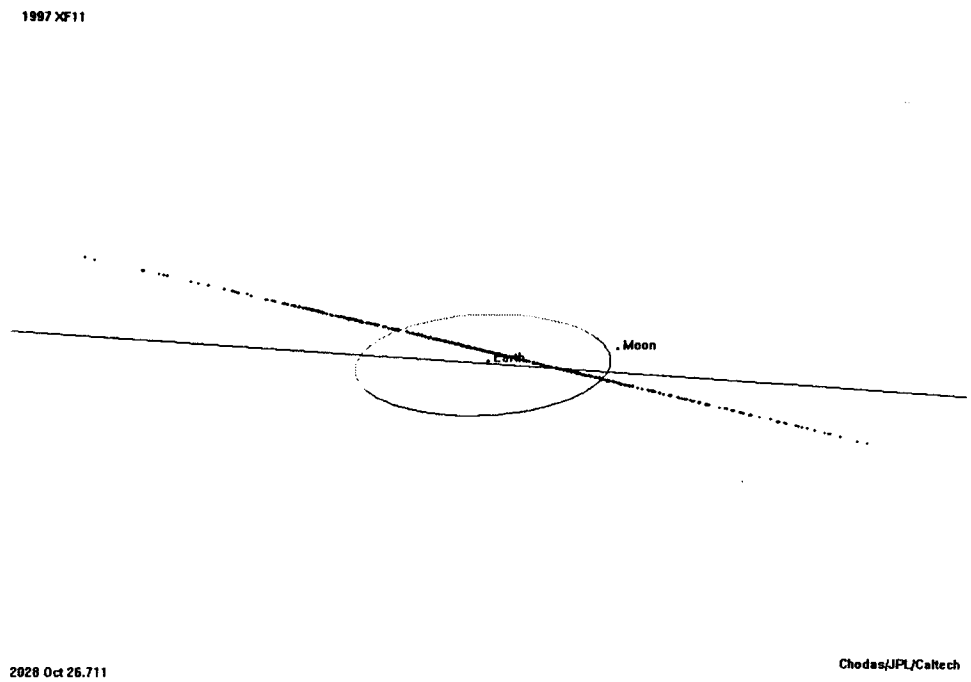

Figure 3 Positions of Monte Carlo points for 1997 XF_{11} at closest approach to Earth in 2028

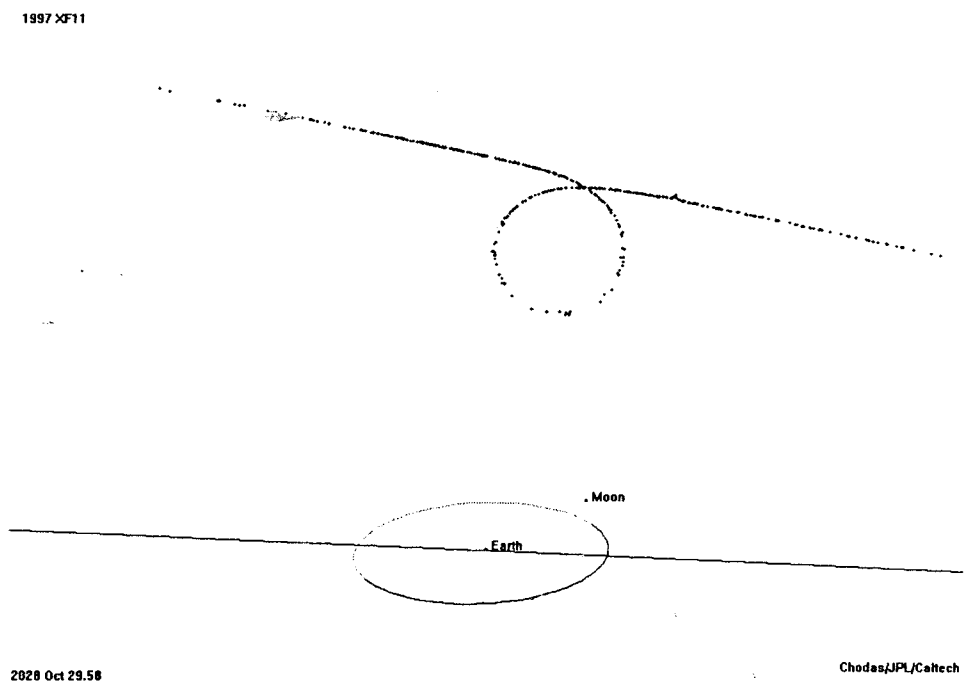

Figure 4 Positions of Monte Carlo points for 1997 XF_{11} 3 days after closest approach to Earth in 2028

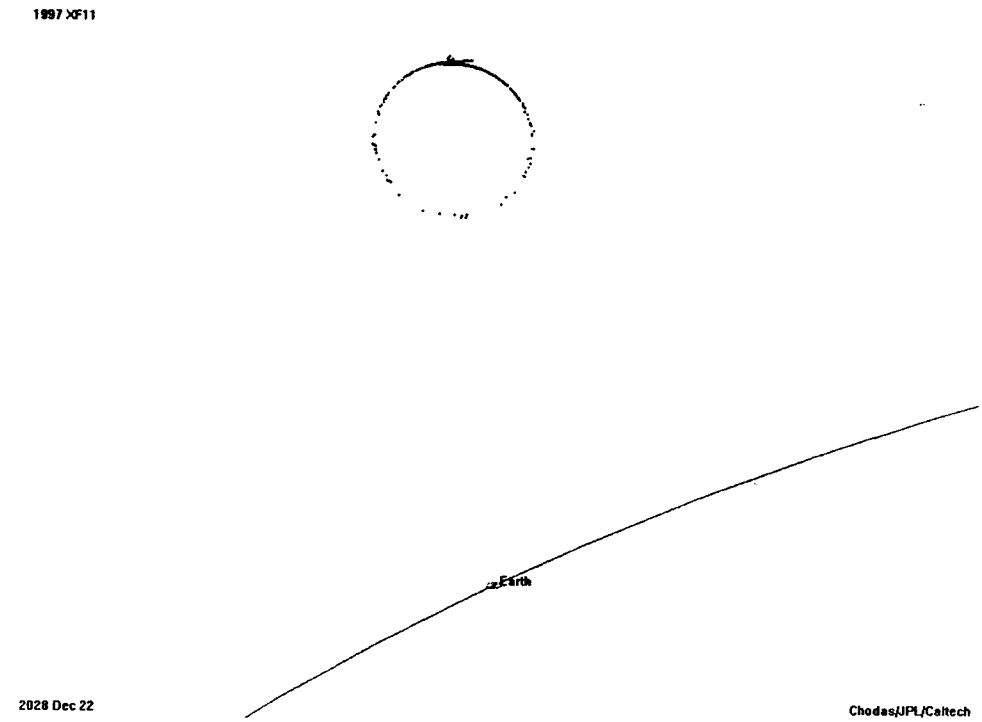

Figure 5 Positions of Monte Carlo points for 1997 XF_{11} 2 months after closest approach to Earth in 2028

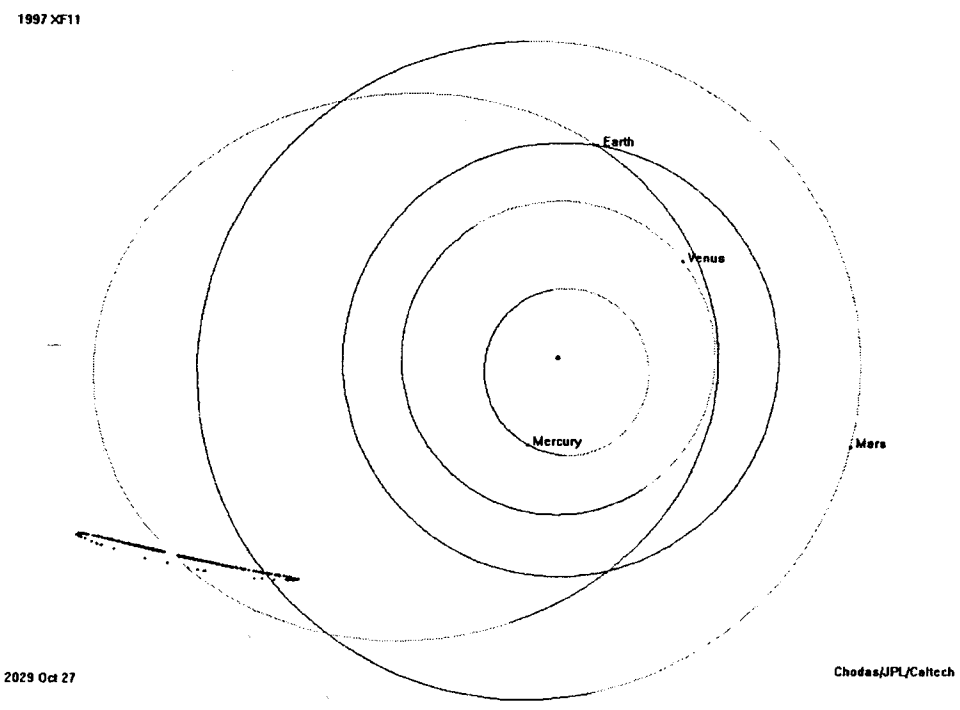

Figure 6 Positions of Monte Carlo points for 1997 XF_{11} 1 year after 2028 closest approach

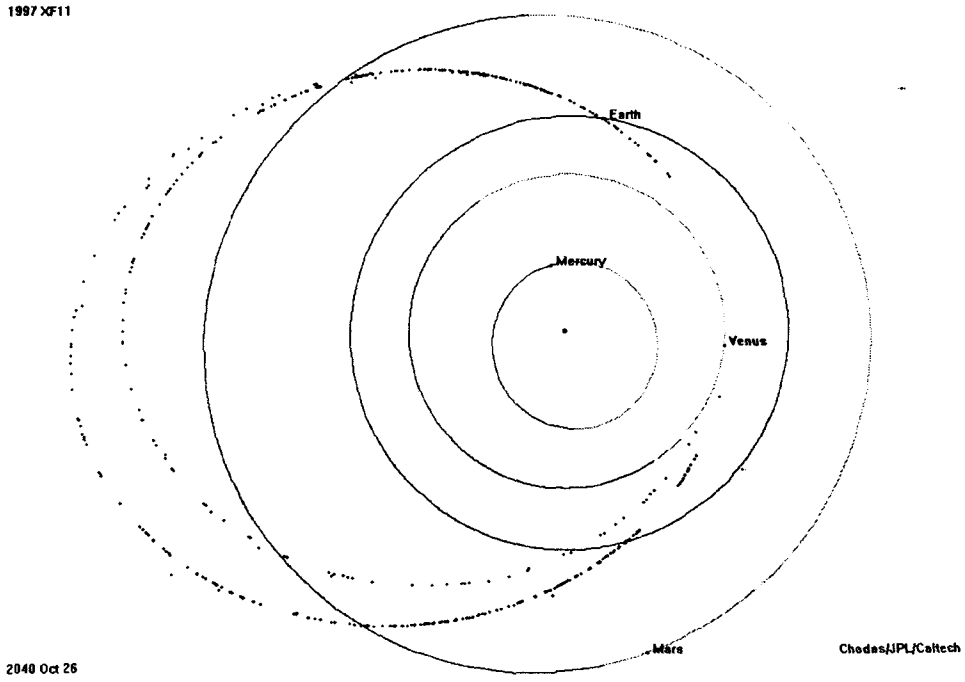

Figure 7 Positions of Monte Carlo points for 1997 XF_{11} in 2040

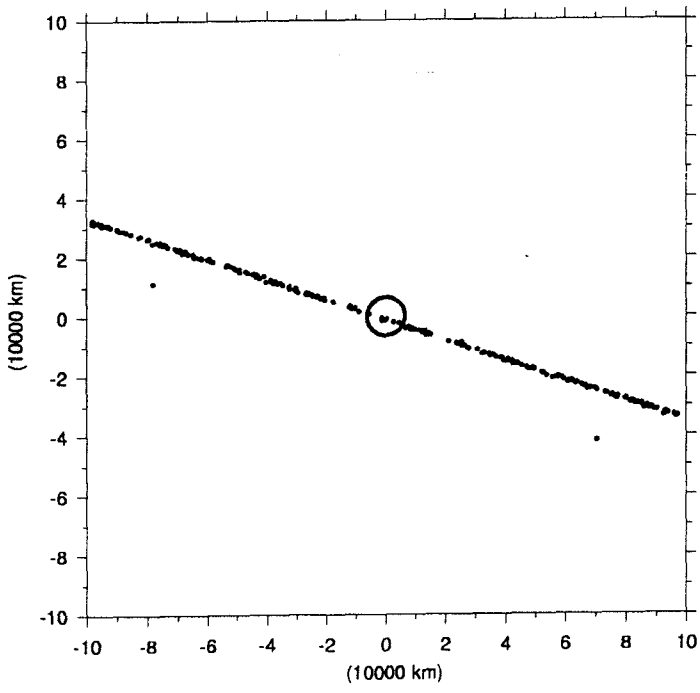

Figure 8 Monte Carlo points for 1997 XF_{11} projected into b-plane for 2040 encounter

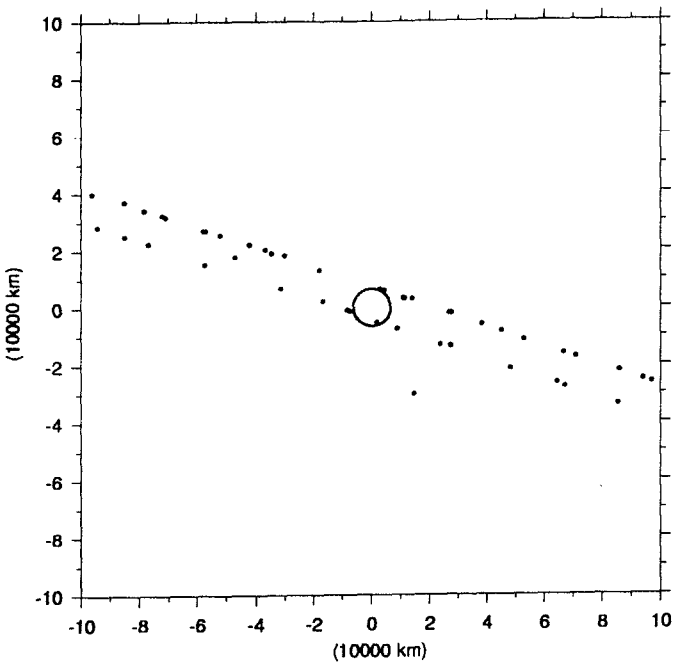

Figure 9 Monte Carlo points for 1997 XF_{11} projected into b-plane for 2041 encounter

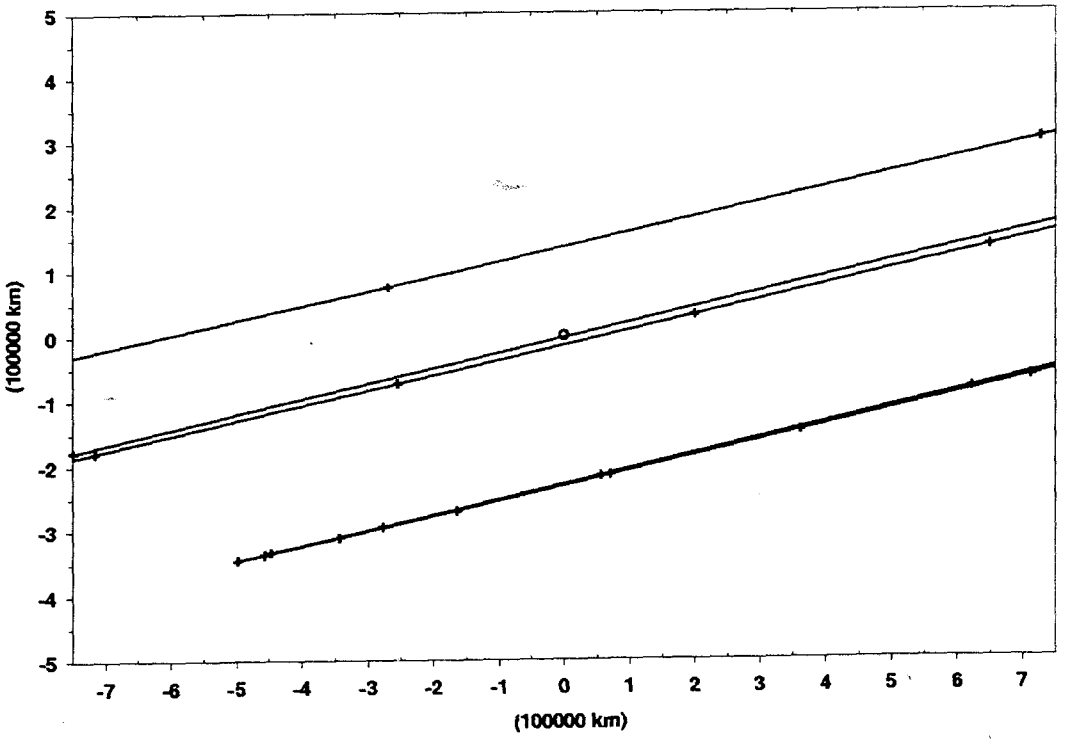

Figure 10 Line of Variation sample points for 1998 OX_4 projected into b-plane for 2046 encounter